Collisional quenching of metastable hydrogen atoms by atoms and molecules*

S. R. Ryan,† S. J. Czuchlewski,‡ and M. V. McCusker§

Physics Department, Yale University, New Haven, Connecticut 06520

(Received 21 March 1977)

The deexcitation or quenching of the metastable $2S$ state of atomic hydrogen in collision with atoms and molecules has been studied using a beam-attenuation method in conjunction with a time-of-flight technique at velocities between 0.4×10^6 and 4×10^6 cm/sec (0.08 and 8 eV). In this regime, transfer of the metastable to the $2P$ state of hydrogen, followed by radiative decay to the ground state, is the dominant destruction mechanism. Absolute cross sections are reported for the quenching of H($2S$) atoms in collision with the noble gases (helium-xenon), with molecules that have permanent electric-quadrupole moments (hydrogen and nitrogen), and with molecules that have permanent electric-dipole moments (ammonia, methanol, and acetone). For molecules with dipole moments, the cross sections are on the order of 10^{-13} cm^2 and vary approximately as v^{-1}. For the noble gases and the quadrupole-moment molecules, the cross sections are on the order of 10^{-14} cm^2 and vary approximately as v^{-n} where $0.3 < n < 0.7$. Measurements of the relative cross section for the production of ultraviolet radiation in collision with nitrogen and argon are reported, and the cross sections for the quenching of H($2S$) and D($2S$) in argon are compared. Data for the noble gases indicate that large-angle elastic scattering is probably not responsible for the discrepancy between theory and experiment. The data for molecular hydrogen suggest that short-range forces are important in collisions with molecules possessing a quadrupole moment.

I. INTRODUCTION

The long-lived $2S$ metastable state of atomic hydrogen is easily deexcited or quenched by collisions with other atoms and molecules. These collisions are of particular interest since the cross section for this quenching process can be calculated from first principles and compared to an absolute measurement of the inelastic scattering. It can be shown using the adiabatic criterion that at low kinetic energies (≤ 50 eV) the physics of the collision is dominated by the presence of the nearby $2P$ states of hydrogen which are nearly degenerate with the $2S$ metastable state. A perturbing electric field during the collision can cause an admixture of the $2S$ and $2P$ states by the Stark effect. After the collision, therefore, there is a finite probability that the hydrogen atom has made a transition to the $2P$ state, in which event the atom decays to the $1S$ ground state emitting a Lyman-α photon. The metastable has thus been quenched (or inelastically scattered) in the reaction

$$H(2S) + X \rightarrow H(2P) + X \rightarrow H(1S) + h\nu + X. \quad (1)$$
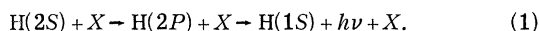
On the other hand, if the atom remains in the $2S$ state after the collision, the metastable will have received a net impulse from the gradient of the electric field during the collision and thus be deflected or elastically scattered. Elastic and inelastic scattering are therefore complementary processes; the relationship between the two depends on the relative velocity in the collision and the nature of the perturbing electric field.

In the low-energy regime where the $2P$ states dominate the inelastic scattering, collisional quenching by the noble gases[1-6] and molecules[7-14] has been studied by several groups. Various theoretical approaches have been employed to calculate these quenching cross sections.[15-19] Many of these same systems have been studied at kinetic energies between 10^2 and 10^4 eV, where additional processes such as excitation to a higher electronic state, ionization, or electron capture are effective in quenching metastables.[20-27]

This paper presents an experimental study of the quenching of metastable atomic hydrogen by low-energy collisions with neutral atoms and molecules using a time-of-flight (TOF) spectrometer. A modified beam-attenuation technique is employed, in conjunction with a highly selective detection scheme, to determine an absolute cross section which depends only on a ratio of intensities and a measurement of length and pressure. This improved technique eliminates many of the problems inherent in a conventional attenuation study and is insensitive to elastic scattering in a collision through angles less than 200 mrad. Cross sections for the quenching of metastable hydrogen are reported for the noble gases (helium through xenon), molecules with a permanent electric-quadrupole moment (hydrogen and nitrogen), and molecules with an electric-dipole moment (ammonia, methanol, and acetone). Sections II and III outline the theory and describe the experimental method. Section IV discusses the cross section for the production of ultraviolet radiation. Sections V and VI present the data and the conclusions, respectively.

II. THEORY

For molecules with a permanent electric-multipole moment, Gersten has developed a time-dependent perturbation theory approach to collisional quenching in which the interaction potential is replaced by the dominant term in the multipole field.[15] The hydrogen atom, initially in the metastable state, is assumed to follow a classical straight-line trajectory. The resulting time-dependent electric field is used to calculate the mixing of the $2S$ and $2P$ states during the collision. The collision can change the rotational state of the molecule, and the total cross section is the sum of the cross sections for all allowed transitions averaged over the initial rotational states of the molecule [Eqs. (14) and (15) of Ref. 15]. In the limit of high temperature and large moment of inertia, this sum reduces to a simple function of the relative velocity v,

$$\sigma_l = \Gamma_l (M_l/v)^{2/(l+1)}, \tag{2}$$

where l is the order of the multipole moment M_l ($l=1$ for dipole and 2 for quadrupole) and Γ_l is a constant. This is the nonadiabatic limit of the theory. At low velocity (and small moment of inertia), it is no longer possible to change the rotational state of the molecule, and the cross section is smaller than predicted by Eq. (2). Slocomb, Miller, and Schaefer also considered quenching by molecules with a permanent multipole field.[16] They use the Born approximation and assume a long-range dipole-multipole interaction. Their results are identical to Eq. (2) with a Γ_l which is a factor of $3^{1/(l+1)}$ smaller than that of Gersten.

In the absence of a permanent electric field, the Stark mixing of the $2S$ and $2P$ states must proceed in terms of shorter-range forces. The cross section for quenching, therefore, might be expected to be small. However, the admixture of $2S$ and $2P$ is appreciable any time the electron cloud of the metastable overlaps that of the atom or molecule. As the metastable is quite large (10% of its charge distribution is outside a radius of 5 Å), the geometric cross section for a collision with a noble-gas atom can easily be on the order of 10^{-14} cm^2.

Two distinct theoretical approaches have been employed to calculate collisional quenching for symmetric atoms such as the noble gases. Byron and Gersten have employed a straight-line trajectory, time-dependent formulation with scattering potentials obtained either by perturbation theory or by a pseudopotential.[17-19] They find that the latter, derived from low-energy-electron elastic scattering, gives better results. The pseudopotential contains a weak, long-range part that includes polarization of the noble gas by dispersion forces and a strong, short-range potential.

Slocomb, Miller, and Schaefer have employed a formalism similar to that of symmetric charge transfer.[16] The quenching cross section in this approach is given by the difference of the amplitude for elastic scattering in the two Born-Oppenheimer Σ states of the excited HX molecule. (X is the spherically symmetric collision partner.) In the separated-atom limit these Σ states correlate to a pure $2S$ or $2P$ hydrogenic state and the ground state of X. At intermediate distances the wave functions correspond to a product of the ground state of X and the linear combination $(2S \pm 2P)$. The quenching is related to the difference in the potential curves for these two states. The required potential curves for these excited states of the HeH molecule were calculated by Slocomb, Miller, and Schaefer, who then used these potentials to determine the quenching cross section. Unfortunately, helium is the only noble gas for which these potentials are known. Olson et al.[6] have inverted the procedure and used the experimental cross sections to calculate the potential difference between these two states in HeH and in ArH. For systems other than He + H($2S$), Slocomb, Miller, and Schaefer have investigated the possibility of using a long-range polarization interaction. In this approximation the cross section varies as $(\alpha/v)^{1/3}$, where α is the polarizability of X.

Elastic scattering, the complementary process to quenching, has received less theoretical attention than its inelastic counterpart. If the interaction potentials are known, the symmetric charge-transfer formalism can be used to calculate the differential elastic scattering cross section.[6] Byron and Gersten have estimated large-angle elastic scattering in the noble gases using the pseudopotential approach. They find that the elastic cross section is typical of a hard-sphere interaction and is characterized by a large peak in the forward direction and a long tail that falls off slowly at large angles. This tail could be important in an attenuation study of quenching. A general feature of the large-angle scattering is that it increases more rapidly with decreasing velocity than the quenching cross section.

It should be noted that quenching processes other than $2S$-$2P$ transitions are possible at low energies in certain systems. A reaction can be important if the net change in the internal energy of the system is less than several tenths of an electron volt. These reactions are of the general form

$$H(2S) + X \rightarrow H(1S) + X^*, \tag{3}$$

where X^* is an excited state (or ion) with an energy approximately 10.2 eV above the ground state. Both krypton and xenon, for example, have excited

atomic states near 10.2 eV. By analogy with excitation transfer in the He(2S) + Ne system, the kinetic energy in the collision might be expected to tune the excitation transfer into resonance. Although the cross section for excitation transfer would have to be large to compete with radiative quenching, such a resonant process could add structure to the attenuation cross section.

III. EXPERIMENTAL METHOD

The cross section for the quenching of a metastable hydrogen atom in a collision with an atom or a molecule is determined by studying the attenuation of a beam of metastables as it passes through a gas of the substance. The beam of metastables is produced in a pulsed manner, and its intensity is determined for a number of different velocities by accumulating a spectrum of the arrival time of the metastables at a detector. The intensity of the beam as measured by a detector at a distance z from the source is given by the formula

$$I(z) = I(0)\Omega(z)e^{-n\sigma z}, \qquad (4)$$

where $I(0)$ is the intensity of the source, $\Omega(z)$ is the product of the efficiency and solid angle of the detector, n is the density of the quenching gas, and σ is the cross section. $I(0)$, σ, and possibly Ω depend on the velocity of the metastable atom. In practice, the intensity is measured at two positions z_1 and z_2 by two separate detectors for several values of n. The cross section is related to the ratio of the intensity at z_1 and z_2 by the equation

$$\ln[I(z_2)/I(z_1)] = \ln[\Omega(z_2)/\Omega(z_1)] - n\sigma(z_2 - z_1). \qquad (5)$$
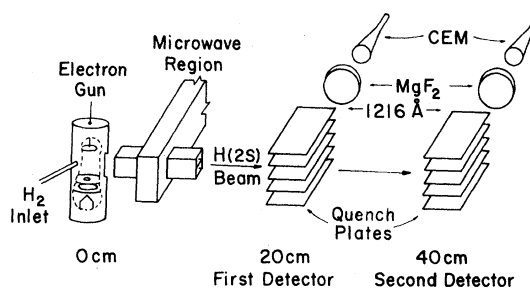
FIG. 1. Schematic of the TOF-beam attenuation apparatus. The electron gun is housed in a water-cooled copper cylinder and consists of an electron collector, a directly-heated pulsed filament, grounded grid, and electron-beam-defining annulus. The metastables enter and exit the microwave region through below-cutoff wave guides set in the cavity walls. The two detectors are shown with only a few of the quench plates. Electrical shields and beam apertures have been omitted. The flight path is open to the vacuum chamber, and the pressure is monitored by ionization gauges.

A least-squares procedure is used to determine the cross section from Eq. (5) for each velocity interval in the TOF spectrum.

A. Apparatus

The apparatus (Figs. 1 and 2) consists of a pulsed source of metastable hydrogen atoms produced by electron-impact dissociation of molecular hydrogen,[28] two metastable-atom detectors at distances of 20 and 40 cm from the metastable source, a microwave cavity that resonantly quenches the metastable atoms to measure background in the beam, a digital clock, and a minicomputer which
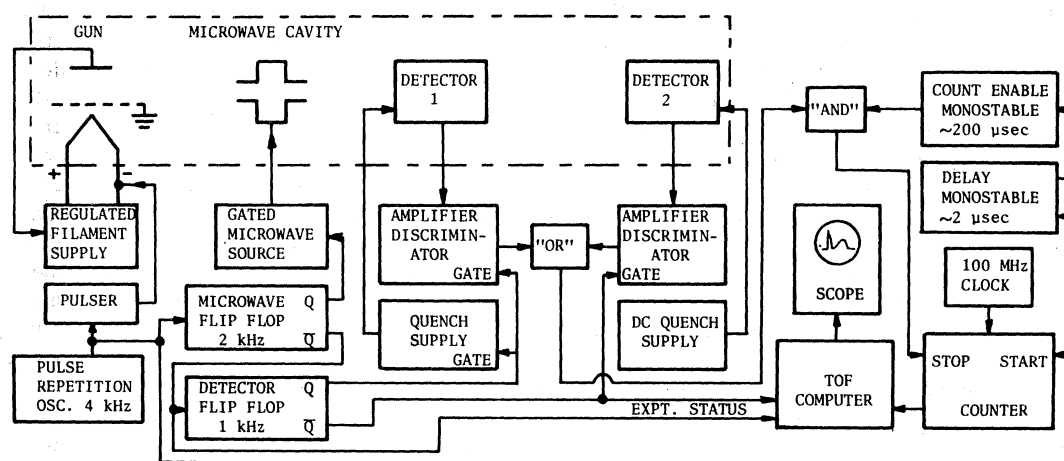
FIG. 2. Block diagram of the experimental electronics. The microwave source is turned on every other gun pulse. Each detector is enabled for two consecutive gun pulses. Stop pulses to the counter are inhibited during the gun pulse. The experimental status lines to the computer determine the memory sector in which the TOF data is stored. The filament current is regulated to ensure a constant metastable production rate. The broken line encloses the actual TOF apparatus.

H(2S) ENERGY (eV)
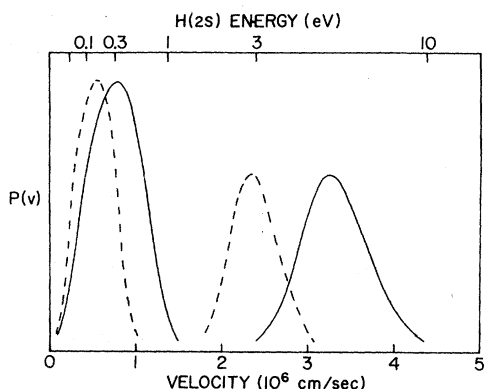
FIG. 3. Velocity distribution of metastable fragments produced by dissociative excitation of molecular hydrogen by electron impact. The solid and dashed curves give the velocity distribution for fragments from H_2 and D_2, respectively.

is programmed as a multichannel analyzer to accumulate the time-of-flight spectrum of the metastable atoms.

In the metastable source an electron gun produces a pulse of electrons (typically 80 eV, 1-mA peak current in a 350-nsec pulse) in a beam at right angles to the metastable beam axis (flight path). These electrons collide inelastically with molecular hydrogen in the source region, leaving a fraction of the molecules in an unbound excited state. These excited molecules subsequently dissociate into two hydrogen atoms some of which may be in the metastable $2S$ state. The velocity distribution of the metastable fragments produced by dissociative excitation of molecular hydrogen or molecular deuterium (Fig. 3) exhibits two peaks corresponding to the dissociation of molecular states associated with two different separated-atom limits. These fragment atoms cover a useful range of velocity from 0.4 to 4.0×10^6 cm/sec (for H_2) with kinetic energy between 0.08 and 8 eV.[10,28,29] The gap between the two groups of metastable atoms will be seen as a break in the cross section data near 1.6×10^6 cm/sec.

After dissociation, the H($2S$) atoms then drift along the flight path with a velocity determined by the kinetic energy released in the dissociation process. When an atom reaches the detector, a static electric field mixes the $2S$ and $2P$ atomic states (Stark effect) making possible a transition to the $1S$ ground state accompanied by the emission of a Lyman-α photon at 1216 Å. This photon is detected by a photomultiplier some time after the gun pulse, and this time is recorded by the computer, which increments the appropriate memory location to accumulate a spectrum of the flight times.

The detector consists of a stack of metal plates connected in a parallel-plate capacitor configura-

tion.[30] This geometry spatially defines the electric field so that the metastable decay is confined to a 0.2-cm distance in front of the leading edge of the plates. The photomultiplier is a channel electron multiplier(CEM) with a 1-cm-diam input cone, which has been coated with a 1500-Å-thick film of potassium iodide to increase the quantum efficiency.[31] The CEM is enclosed in a shielded box and the input cone is operated at ground potential to reduce sensitivity to charged particles in the beam. The CEM is separated from the parallel-plate array by a MgF_2 window, which provides a short-wavelength cutoff and blocks particles. The window is covered with a fine wire mesh to prevent accumulation of charge on the MgF_2. The CEM is operated in a pulse-counting mode. The output pulse is amplified and discriminated to ensure constant detection efficiency. When zero voltage is applied to the parallel-plate array of the first detector on the flight path, the beam is free to proceed to the second detector.

Although the detection scheme is highly selective, photons and charged particles created in the metastable source constitute a background that is approximately 10% of the metastable count. To measure this background the metastable beam is passed through a microwave electric field at the $2S_{1/2}$-to-$2P_{3/2}$ transition frequency (9.9 GHz) to resonantly quench the metastable beam before it reaches either detector. Photons and charged particles are unaffected by the field. Spectra are accumulated with and without the microwave field and later subtracted to eliminate the background completely.

Four separate TOF spectra are accumulated at the same time in the following manner. To initiate a data cycle, the electric field at the first detector and the microwave field are turned on. The electron gun is pulsed, starting a digital scaler that counts a 100-MHz clock. If an H($2S$) atom is detected at the first detector, the counter is stopped and the computer increments the appropriate time-of-flight channel in the segment of memory corresponding to background at the first detector. The microwave field is turned off, and the gun pulsed again. An event, if it occurs, is stored in a second TOF spectrum by the computer. The quench field at the first detector is turned off and the process repeated for the second detector. The electron gun is pulsed at a rate of several kilohertz to accumulate the four TOF spectra.

The experiment is contained in a 225-liter, cylindrical, stainless-steel vacuum chamber, which is evacuated by a 23-cm(9-in.) mercury diffusion pump with an effective pumping speed for nitrogen of 400 liter/sec at the chamber. A mercury pump was chosen to avoid the accumulation of a charged, insulating film of oil that could quench metastable

hydrogen atoms. A liquid-nitrogen trap and a re-
frigerated chevron baffle at −35 °C enable the sys-
tem to reach an ultimate vacuum of 3×10^{-8}
torr.
When gases such as xenon or methanol are studied,
the liquid-nitrogen trap is operated with a dry ice
and alcohol mixture. The vapor pressure of these
gases when frozen on a trap filled with liquid ni-
trogen is high, and the net pressure in the chamber
varies with the coolant level in the trap.

B. Attenuation-ratio method

The technique of using the ratio of intensities
(attenuation ratio) to determine the cross section
has many advantages. The cross section measured
in this manner is absolute and depends only on a
ratio of intensities and a measurement of pressure
and distance. The technique is inherently capable
of high accuracy and is relatively insensitive to
large-angle elastic scattering. Since the four TOF
spectra are accumulated at the same time, the at-
tenuation-ratio is insensitive to fluctuations in ex-
perimental parameters such as metastable produc-
tion rate. The high selectivity of the detector and
the method of subtracting background enables the
measurements to be extended with confidence to
the wings of the metastable velocity distribution,
where the counting rate is low. The cross section
is independent of the efficiency of the detectors as
long as the efficiency remains constant during a
run. This condition is ensured by comparing TOF
spectra taken at zero scattering-gas pressure be-
fore and after each series of runs that constitute
a cross section measurement. In fact, since these
spectra define the zero-pressure attenuation of the
metastable beam, they are included in the least-
squares determination of the cross section.

The gas density along the flight path is given by
the pressure in the vacuum chamber, which is
measured by two ionization gauges. The gauges
are operated at reduced emission current to en-
sure linearity at high pressure. They are calibra-
ted before and after a cross-section measurement
by comparison with a capacitance manometer at
pressures between 5×10^{-6} and 5×10^{-4} torr. The
uncertainty for this procedure was 3% for the per-
manent gases. The capacitance manometer (ac-
curacy better than 1%) was calibrated by the manu-
facturer against a primary standard during the
course of this work. The purity requirements for
the scattering gas are modest and are easily met
using gas from commercial cylinders (dew point
of −30 °C or lower) without further purification.
Gases of methanol and acetone were produced by
drawing the vapor above a temperature-stabilized
liquid sample through a needle valve into the va-
cuum chamber. The uncertainty in the pressure
calibration for these substances is approximately 8%.

A drift in the pressure, and therefore the den-
sity, of the scattering gas during a run will intro-
duce an error in the cross section. However, the
error in the attenuation ratio is second order in
the pressure variation if the time average of the
density is used in the least-squares analysis. This
can be shown by considering the integral with re-
spect to time of the beam intensity (Eq. 4) which is
equal to the number of metastables N detected at
z after a time T,

$$N(z) = \int_0^T I(z)\, dt$$

$$= I(0)\Omega(z)e^{-\bar{n}\sigma z} \int_0^T e^{-\sigma z[n(t)-\bar{n}]} dt, \tag{6}$$

where $\bar{n}$ is the time average of the density $n(t)$ over
the time interval 0 to T. The integrand may be ex-
panded in a power series and integrated. By de-
finition of $\bar{n}$, the integral of the term linear in
$[n(t)-\bar{n}]$ is identically zero. Consequently the first
nonzero correction is proportional to the mean-
square variation in density from its time-average
value (i.e., the variance). A typical variation of
10% in the density, therefore, introduces an error
of 1% in the attenuation ratio. The least-squares
analysis further reduces this error since a drift
in the pressure during one run is not correlated
with another.

Molecular hydrogen effusing from the source at-
tenuates the metastable beam. Because the source
pressure is nominally fixed during a cross-section
measurement, this attenuation is constant and con-
tributes to the zero-pressure attenuation of the
metastable beam. However, the quenching cross
section for hydrogen is measured in this study,
and it is a simple matter to correct the attenuation
ratio for any small variation in the source pres-
sure during a series of runs. This correction,
which is typically less than 3%, is made in data
analysis.

A systematic error is introduced by the digital
clock which counts only the first event after the gun
pulse. This discriminates against slower meta-
stables. Low counting rates make this effect
small; however, it is possible to eliminate the er-
ror completely. At a given time-of-flight, the to-
tal number of events in that channel is equal to the
number of counts recorded by the system divided
by the quantity $(1-P)$ where P is the probability
that the clock had been stopped by a prior event.
This probability is just the total number of events
accumulated in earlier TOF channels divided by
the total number of gun pulses. The TOF spectra
are corrected channel by channel for this distor-
tion in data analysis.

The elastic scattering of a metastable through an

angle large enough such that it misses the detector would be interpreted as quenching in an attenuation experiment and would increase the measured cross section. Although elastic scattering in the noble gases is strongly peaked in the forward direction, scattering through angles greater than 30 mrad is predicted to be comparable to the collisional quenching.[19] Since elastic collisions occur along the entire flight path, no simple geometric consideration will characterize the angular acceptance of the detector. The problem is further complicated by the fact that only those metastables that are detected by the first detector and missed by the second are important. It is possible, however, to estimate the effective acceptance angle of the detection system by integrating the elastic attenuation of the beam along the flight path using a model[19] for the differential cross section. The average cross section computed from this attenuation can then be compared to the integral of the differential cross section to determine an effective acceptance angle. This procedure shows that repopulation of the beam by small-angle elastic scattering substantially reduces the net elastic attenuation of the beam; that is, metastables originally outside the solid angle of the detector can be scattered into the beam. In the absence of beam-limiting apertures along the flight path, repopulation of the beam will completely compensate for scattering out of the beam if the differential cross section is strongly peaked in the forward direction. Introducing appropriate experimental geometry, the calculation shows that the metastable beam arrives at the first detector essentially unattenuated and that repopulation of the beam reduces the elastic attenuation between the two detectors by 35% or more. The effective acceptance angle of the detection system estimated by this method is greater than 200 mrad and increases as the ratio of large-angle to small-angle scattering increases. Repopulation of the metastable beam slightly increases the flight path and leads to a small amount of velocity averaging in the cross section. Changing the mass of the collision partners changes the laboratory scattering angle as well as the center-of-mass differential cross section. The first effect, which is easily examined by the above procedure, reduces the elastic attenuation of a D(2S) beam relative to an H(2S) beam by 2% in H_2, 0.5% in He, and 0.3% in Ar. The attenuation in Ar is 8% larger than in He.

IV. ULTRAVIOLET-PRODUCTION CROSS SECTION

A simple modification of the experimental procedure makes it possible to measure the relative cross section for the production of ultraviolet radiation by collisions. Since the collision-induced transition from the 2S to the 2P state is the dominant quenching mechanism below 50 eV, the ultraviolet light produced in a collision will be predominately Lyman-α radiation, and the radiation-production cross section will, in general, be equal to the total inelastic-scattering cross section. In contrast to an attenuation measurement, this measurement is inherently free from the effects of elastic scattering.

In this mode of operation, a single detector is employed, and the electric field on the detector quench plates is alternated on and off. The TOF spectrum collected in the presence of the field measures the metastable-beam intensity while the zero-field spectrum is proportional to the quenching along the portion of the flight path in front of the photodetector. The ratio of counts in the two spectra (typically 2%) yields the fraction of metastables quenched by collisions. This quenching fraction is then measured as a function of gas density, and the relative cross section is extracted by a least-squares analysis in the same manner as the attenuation-ratio technique.

The effective length along the flight path seen by the photodetector (nominally 1 cm) is not accurately defined. It is complicated by a possible variation of the quantum efficiency of the photodetector as the angle of incidence of the photon on the cone of the CEM changes with the position of metastable decay along the flight path. The uv-production cross section therefore is a relative cross section and should be normalized to the attenuation-ratio cross section at a velocity where the elastic scattering is negligible. This normalization factor can then be applied to all collision partners as the effective path length is independent of quenching gas.

The poor spatial resolution of the detector (approximately 1 cm) when operated in the absence of an electric field can introduce a systematic error in the cross-section measurement. If the TOF spectrum has sharp structure such that adjacent channels vary greatly in the number of counts (e.g., the fast group of metastables), the effect of this poor resolution will be to shift a fraction of the metastables from the channel with a high count to an adjacent channel with fewer counts thereby distorting the quenching fraction. The cross section measured on the wings (peak) of the fast group of metastables will therefore be increased (decreased). This distortion is minimal in the velocity range covered by the slow metastable group. To normalize the uv cross section in nitrogen at a high velocity where any elastic scattering would be small, all of the TOF channels in the fast group were combined to determine an average cross sec-

tion which was then compared to the attenuation-ratio measurement.

V. DATA AND DISCUSSION [a]

The TOF spectrum is divided into 500 channels of width 350 nsec. The spectrum from the first detector is scaled in time to that of the second detector and channels are combined when the uncertainty in time is less than that in the flight path. The finite pulse and channel width yield a 6% uncertainty in the velocity at 4×10^6 cm/sec; the 1.5% uncertainty in the flight path dominates at low velocity. The cross sections are thus averaged over a velocity interval approximately equal to the separation between data points.

The attenuation ratio is determined at some 60 velocities for typically five different pressures of quenching gas between 0.2 and 20×10^{-5} torr. This data, along with the two zero-pressure ratios, is fitted to Eq. (5) by a linear, least-squares procedure to determine the cross section. The error in the cross section is calculated by the fitting program and represents an uncertainty of one standard deviation in the value of the slope of Eq. (5). The uncertainty in the fit for an individual datum, indicated by representative error bars in Figs. 4–13, ranges from ±2% to ±15% and is dominated by the statistical uncertainty in the TOF spectrum. These error bars do not reflect an overall 3% (8%) uncertainty in the cross section due to the pressure calibration for the permanent (condensable) gases.

As an aid to the normalization and comparison of cross sections, the data were fitted to two different functional forms:

$$\sigma = A_0 + A_1 \ln(v) + A_2 [\ln(v)]^2 + A_3 [\ln(v)]^3 \quad (7)$$

and

$$\sigma = \sigma_0 v^{-n}, \quad (8)$$

where the A_i or σ_0 and n are determined by a least-squares procedure. Table I gives the value of these parameters for each gas. In general Eq. (7) provides a better fit to the data and is indicated by a solid curve through the data points in Figs. 4–11. The kinetic energy indicated in Figs. 4–13 is measured in the laboratory frame of reference.

The TOF measurement of the cross section assumes that the quenching gas is static and not in random thermal motion. At the hyperthermal velocities encountered in this experiment, the thermal motion is important only in hydrogen and helium at the lowest velocities reported. If the cross section varies as a power of the velocity, it is possible to correct the measured cross section for the thermal motion of the quenching gas.[32] The dashed line slightly below the solid curve in the He (Fig. 4) and the H_2 (Fig. 10) data indicates the corrected cross section.

A. Noble gases

The cross sections for the quenching of metastable hydrogen in collision with the noble gases are shown in Figs. 4–8 where the points and circles are the result of the present study, the triangles indicate the work of Kass and Williams,[1,2] and the crosses represent the data of Dose and Hett.[6,14] The squares indicate an effective cross section (quenching plus elastic scattering through angles greater than 30 mrad) calculated by Byron and Gersten[19] for the work of Kass and Williams.

The cross section for helium is shown in Fig. 4 where the dotted curve is the symmetric charge-exchange calculation of Slocomb, Miller, and

TABLE I. Coefficients for functional representation of cross sections, [a] Eqs. (7) and (8).

Collision partner	σ_0	n	A_0	A_1	A_2	A_3
He	85	0.37	83.94	−30.36	8.30	−2.63
Ne	68	0.40	67.26	−25.60	6.64	−2.38
Ar	84	0.48	92.48	−44.84	22.02	−6.25
Kr	114	0.57	103.97	−76.61	49.14	−12.75
Xe	169	0.66	161.78	−128.88	52.57	−1.75
H_2	93	0.34	90.87	−29.25	12.62	−6.48
N_2	147	0.56	143.53	−92.16	30.38	0.07
N_2 (relative)[b]	148	0.56	127.27	−80.76	51.09	−15.81
NH_3	825	0.80	833.17	−608.29	265.91	−92.46
$(CH_3)_2CO$	1417	0.91	1699.23	−1250.94	20.20	+186.11
CH_3OH	657	0.79	727.17	−462.98	42.62	+12.64

[a] Cross section and velocity measured in units of 10^{-16} cm^2 and 10^6 cm/sec, respectively.
[b] Relative cross section in nitrogen has been normalized to the absolute cross section at 3.1×10^6 cm/sec.
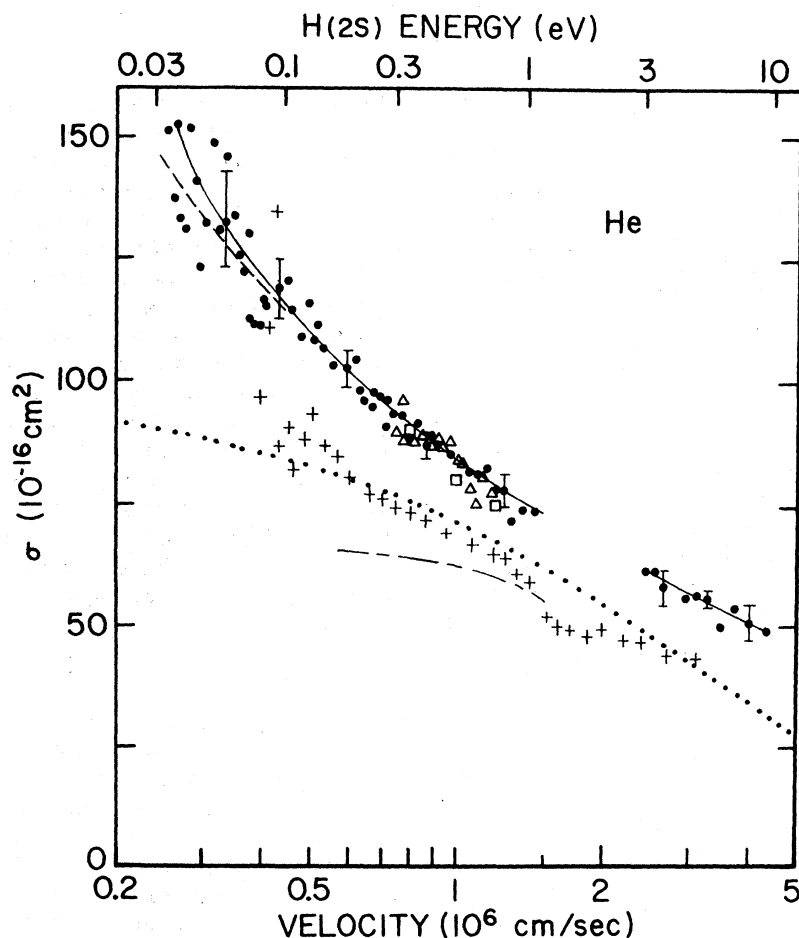
FIG. 4. Cross section for quenching in He. The points, triangles, and crosses are the data from the present study, Kass and Williams, and Dose and Hett, respectively. The solid curve is a fit of Eq. (7) to the data, and the dashed curve indicates the cross section corrected for thermal motion of the target gas. The dotted and broken curves are the theories of Slocomb, Miller, and Schaefer and Byron and Gersten, respectively. The open squares are the effective cross section calculated by the latter for the work of Kass and Williams.

Schaefer[16] and the broken curve represents the pseudopotential treatment of Byron and Gersten.[19] Both calculations are lower than the data presented here and differ dramatically in the low-velocity behavior. An earlier experimental study by Comes and Wenning[33] (not shown) yields a cross section of 8×10^{-16} cm² at 0.35×10^6 cm/sec, which is considerably smaller than all subsequent work.

The cross section for quenching in argon (Fig. 5) was measured using a mixture of H_2 and D_2 in the dissociation source. The insert in Fig. 5 illustrates the results of a preliminary investigation of the relative cross section for the production of ultraviolet radiation in Ar. This cross section has been normalized to the attenuation-ratio data (solid curve in insert) at 1×10^6 cm/sec. This cross section was determined using $H(2S)$ metastables at one argon pressure and has a large statistical uncertainty at the lowest velocities. The agreement in the velocity dependence of these cross sections above 0.5×10^6 cm/sec is good and argues against a large elastic-scattering contribution to the data.

The attenuation-ratio cross section in Ar above

1×10^6 cm/sec is shown in Fig. 6; this figure also indicates the percentage of $H(2S)$ in the combined TOF distribution. Near 2×10^6 cm/sec the cross section is measured using a pure $D(2S)$ spectrum, while at somewhat higher and lower velocity the cross section is determined using only $H(2S)$. To check the hypothesis that the quenching is independent of nuclear mass, the regions of pure $H(2S)$ and $D(2S)$ were separately fitted to Eq. (7) by a least-squares procedure. The fit is indicated by the solid curve in each region. An interpolation of the H data (dashed curve) through the D region suggests an 8% difference in the $H(2S)$ and $D(2S)$ cross sections. This difference, which is comparable to the statistical uncertainty for an individual datum, cannot be accounted for by elastic scattering given the good agreement in the velocity dependence of the attenuation-ratio and uv-production cross sections. It is interesting to note that the 8% difference disappears when metastables of the same center-of-mass kinetic energy are compared (vertical arrows connected by a horizontal line in Fig. 6).
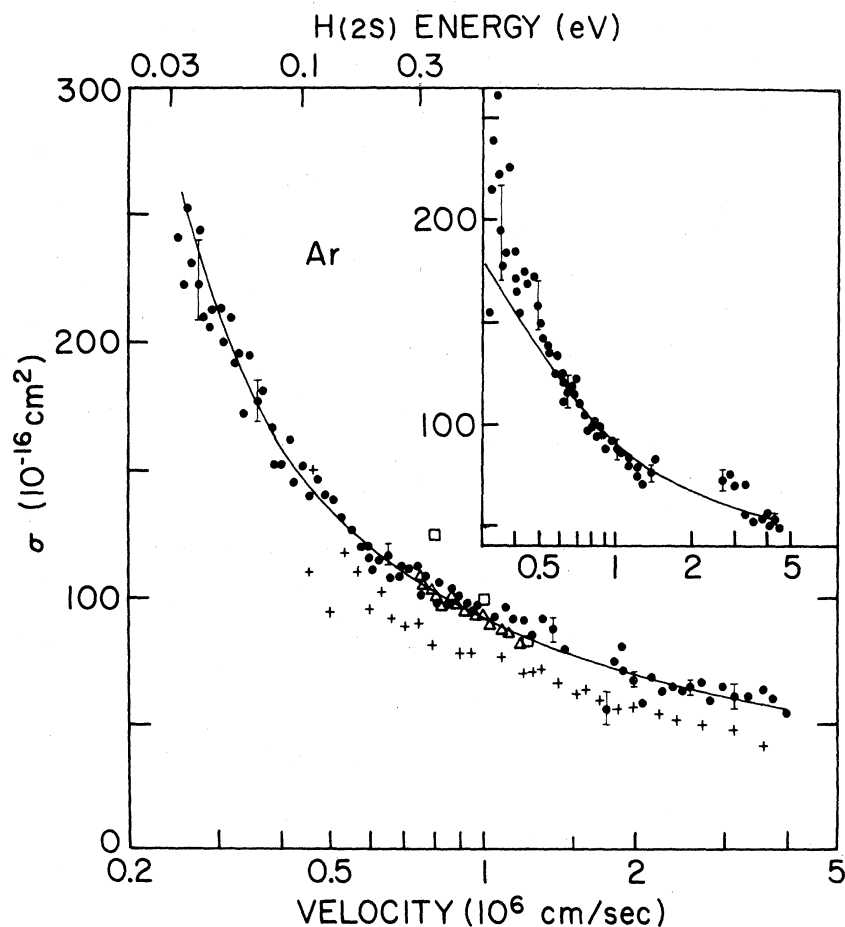
FIG. 5. Cross section for quenching in argon using H and D metastables. The points, triangles, and crosses are the data from the present study, Kass and Williams, and Dose and Hett, respectively. The open squares are the effective cross section calculated by Byron and Gersten. The data in the insert are the relative cross section for the production of Lyman-α radiation in a collision with argon and have been normalized to the attenuation-ratio cross section (solid curve) at 1×10^6 cm/sec.
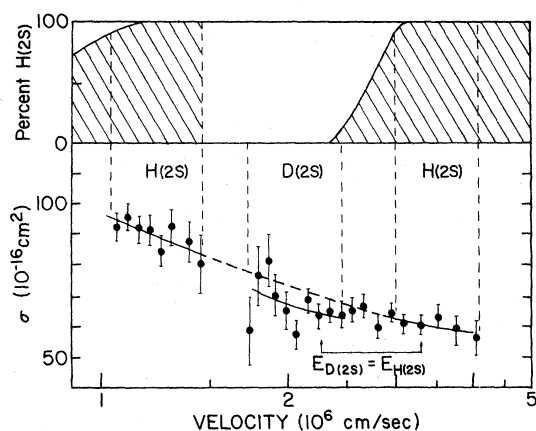
FIG. 6. Comparison of the cross section for quenching of H(2S) and D(2S) in argon. The graph at the top shows the percent of H(2S) in the velocity distribution. The solid curves in the H(2S) and D(2S) regions (indicated by vertical dashed lines) are a fit of Eq. (7) to the data in each region. The H(2S) curve is interpolated through the D(2S) interval and indicates a possible 8% difference in quenching for the two isotopes. This difference is not evident when metastables of the same energy are compared (vertical arrows connected by horizontal line).

The cross sections for quenching in neon and krypton are indicated by the solid and open points respectively in Fig. 7. The data for xenon is shown in Fig. 8. The effective cross section for krypton (open squares) predicted using the pseudopotential approach is slightly higher and rises more rapidly at low velocity than the experimental data. The data for Kr and Xe show no evidence of collisional transfer of excitation between the metastable and these noble gases.

Data for all the noble gases are compared in Fig. 9(a). To check the simple model for quenching based on the polarizability α, which predicts a cross section proportional to $(\alpha/v)^{1/3}$, the data is scaled by $\alpha^{1/3}$ (relative to argon) in Fig. 9(b). A velocity dependence of $v^{-1/3}$ is also indicated. It is clear that the polarization model is too simple and that shorter-range forces are important.

Collisional quenching in the noble gases has also been studied by Kass and Williams who used a conventional beam-attenuation method with a 30-mrad acceptance angle and metastables produced by electron impact on thermally dissociated hydrogen.[1,2] Their measurements in He, Ar, and
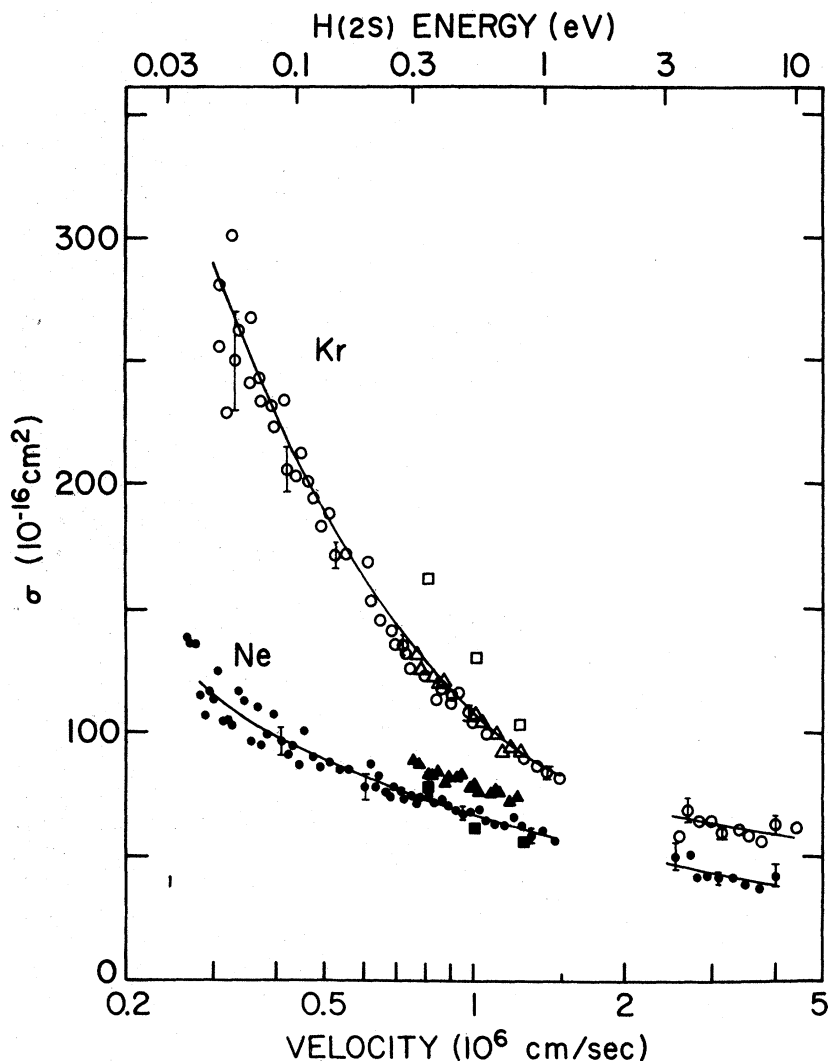
FIG. 7. Cross section for quenching in Ne (solid points) and Kr (open points). The circles are the result of the present study, and the triangles the work of Kass and Williams. The squares are the effective cross sections of Byron and Gersten.

Kr agree well with the data reported here. The only discrepancy is in neon where the cross sections differ by 12%. The agreement between these two studies argues against the large elastic scattering predicted by the pseudopotential approach. Since the effective acceptance angle of the present detection system is approximately six times the angle used by Kass and Williams, the elastic contribution to this work should be significantly reduced. Thus, if the effective cross sections of Byron and Gersten were correct, there would be a discernible difference between the two studies.

Dose and Hett used a conventional beam-attenuation method with a 90-mrad acceptance angle to study metastable collisions. The slightly lower cross sections that they report might suggest the presence of elastic scattering in the other two studies were it not for the substantial agreement in the velocity dependence of the cross sections. Olson et al.[6] report a relevant calculation using the Slocomb, Miller, and Schaefer formalism in which they find the elastic scattering in helium (at angles greater than 90 mrad) to be negligible at 4 eV, increasing to 25×10^{-16} cm^2 at 0.1 eV.

The cross sections measured by Dose and Hett in the noble gases and in molecular hydrogen and nitrogen are consistently 12% to 15% lower than the values reported here. This discrepancy, which is independent of the nature of the quenching gas and the metastable velocity (except perhaps at the lowest velocities), is probably the result of a systematic error such as in the determination of the effective density of the quenching gas. At the lowest velocities, the cross sections reported by Dose and Hett increase more rapidly than the present work. This is particularly evident in xenon. Since the effective acceptance angle of the detection system used in this work is probably twice that reported by Dose, it is possible that this relative increase at low velocity is due to elastic scattering.
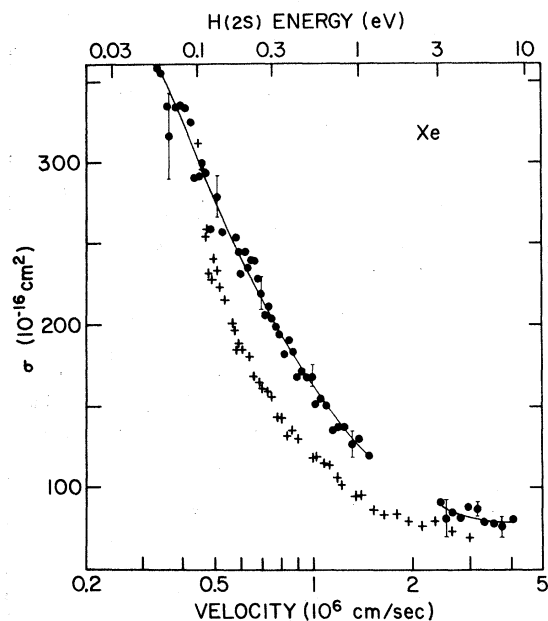
FIG. 8. Cross section for quenching in Xe. The dots are the result of the present study, and the crosses the work reported by Dose.

Dose cites evidence that would support this interpretation.[14] Dose and Hett have used a mixture of H_2 and D_2 in the metastable source for most of their work. Our previous work on dissociative excitation is in slight disagreement with their data
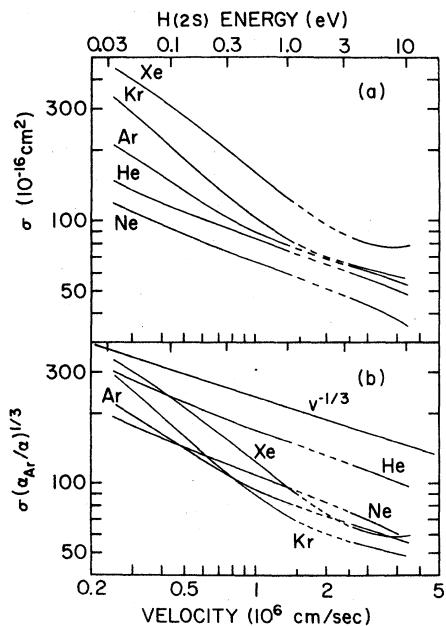
FIG. 9. (a) Comparison of cross sections for the noble gases. (b) Cross sections for the noble gases scaled by the cube root of the polarizability (relative to argon). A velocity dependence of $v^{-1/3}$ is also indicated.

in that we find a gap in the combined H-D TOF spectrum near 1.6×10^6 cm/sec.[10,29]

B. Molecules with quadrupole moments

The cross section for collisional quenching by molecular hydrogen, which has permanent electric-quadrupole moment,[34] is shown in Fig. 10 where the points indicate the present work, and the crosses a measurement by Dose and Hett.[5] The broken curve below the experimental data is the prediction of the perturbation theory approach developed by Gersten.[15] Because collision-induced rotational transitions are unlikely at low velocity in molecular hydrogen, this cross section lies below the nonadiabatic limit of the theory [Eq. (2), dotted curve]. The open square indicates the magnitude of the cross section calculated by Slocomb, Miller, and Schaefer[16] which has the same velocity dependence as the dotted curve. The datum (triangle) at 8×10^5 cm/sec is a velocity-averaged cross section measured by Fite et al.[7] The agreement with the present work is perhaps slightly fortuitous since their correction for the anisotropy of Lyman-α radiation in their detector is uncertain.

Dose and Hett have reported a study of the production of Lyman-α radiation in H_2 which is similar to the quenching-fraction method except that
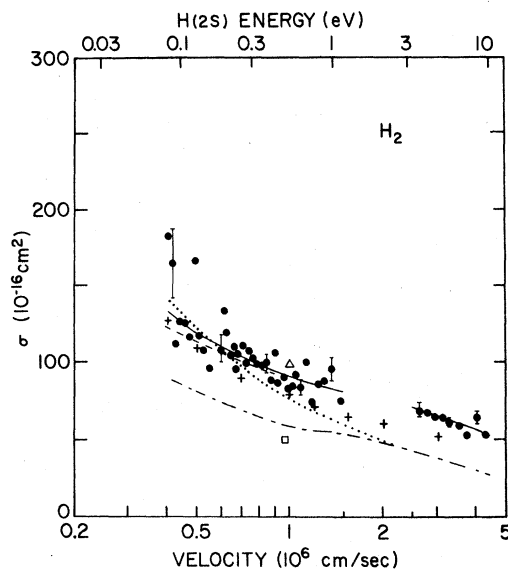
FIG. 10. Cross section for quenching in H_2. The points are the results of the present study and the crosses the work of Dose et al. The solid curve is a fit of Eq. (7), and the dashed curve the cross section corrected for thermal motion. The broken curve is the prediction of Gersten's full theoretical treatment, while the dotted curve is his theory in the nonadiabatic limit. The open square is a calculation by Slocomb, Miller, and Schaefer and the triangle a measurement by Fite et al.

an independent measurement of the attenuation cross section is used to analyze the data.[13] They find that the relative Lyman-α cross section has the same velocity dependence as their absolute attenuation cross section.

Not shown in Fig. 10 are cross sections of 68 $\times 10^{-16}$ cm^2 for H(2S) on H$_2$ and 141×10^{-16} cm^2 for D(2S) on D$_2$ (at 0.35×10^6 cm/sec) reported by Comes and Wenning who studied the Lyman-α fluorescence in a photodissociation experiment.[33] Earlier they reported a radiationless process which accounted for half of the quenching and a total cross section which increased with velocity.[35] The velocity dependence and the magnitude of their total cross section is in complete disagreement with both the present work and that of Dose and Hett. Mentall and Gentieu, in a similar experiment, observed a radiationless quenching process that accounts for one quarter of their total cross section.[36] The radiationless quenching observed in these experiments, however, is extremely sensitive to the correction for the anisotropy of the Lyman-α radiation in an electric field and should be viewed with some caution.

The possibility of a radiationless cross section with a velocity dependence similar to the Lyman-α cross section is not eliminated by the work of Dose and Hett. It would be a possible explanation for the difference between the present work and Gersten's theory.[37] However, the most likely reason for the discrepancy is the presence of a short-range force which is not included in the theory. Since quenching in He is comparable to that in H$_2$, it is clear that the short-range forces effective in the noble-gas collisions are large enough to compete with the small quadrupole field of H$_2$.

The cross section for quenching in nitrogen is shown in Fig. 11. The triangle is a velocity-averaged cross section measured by Fite et al.,[7] and the cross a value reported by Dose and Hett who indicate a velocity dependence in agreement with theory.[11] The broken curve is the prediction of the quadrupole quenching theory in the nonadiabatic limit, Eq. (2), using Gersten's value of Γ_2. If Gersten's Γ_2 is correct, the agreement between theory and experiment indicates that the quadrupole field of nitrogen is large enough to quench effectively beyond the range of any short-range force. The Slocomb, Miller, and Schaefer value of Γ_2 yields a cross section (open square) 30% smaller than Gersten's.

The insert (Fig. 11) shows the uv radiation production cross section measured by the quenching-fraction technique. The dashed and solid curves indicate the fit of Eq. (7) to the quenching-fraction and attenuation ratio data, respectively. The uv cross section has been normalized at 3.1×10^6 cm/
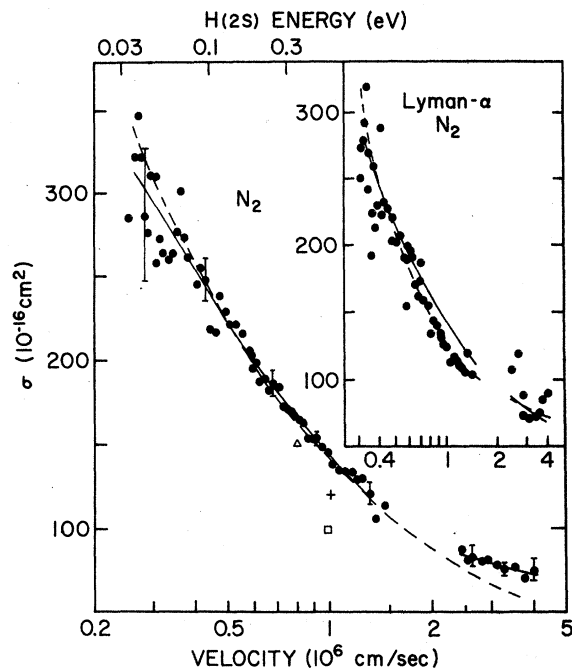
FIG. 11. Cross section for quenching in N$_2$. The dots are the result of the present study; the triangle is a velocity-averaged measurement by Fite et al., and the cross is a value reported by Dose and Semini. The solid curve is a fit of Eq. (7) to the data and the dashed curve the prediction of Gersten's theory in the nonadiabatic limit. The open square indicates the magnitude of the Born-approximation cross section predicted by Slocomb, Miller, and Schaefer. The relative cross section for the production of Lyman-α radiation is shown in the insert. The dashed and solid curves in the insert represent the fit of Eq. (7) to the quenching-fraction and attenuation-ratio data, respectively. The data are normalized at the fast peak.

sec (the peak of the fast metastable group) by combining all TOF channels in the fast group and determining an average cross section. The two cross sections have an almost identical velocity dependence which would eliminate elastic scattering or a radiationless quenching process that did not have a similar velocity dependence.

C. Molecules with dipole moments

Molecules with a permanent electric dipole moment[38] are very effective in quenching metastable hydrogen atoms. Cross sections for ammonia (Fig. 12) and methanol and acetone (points and circles, respectively, in Fig. 13) were measured as an adjunct to a study of dissociative excitation in these molecules. These data are subject to an 8% uncertainty in pressure measurement. Individual ratio measurements were subject to a maximum uncertainty of 4% due to pressure fluctuation. Typically, the attenuation ratio was measured at
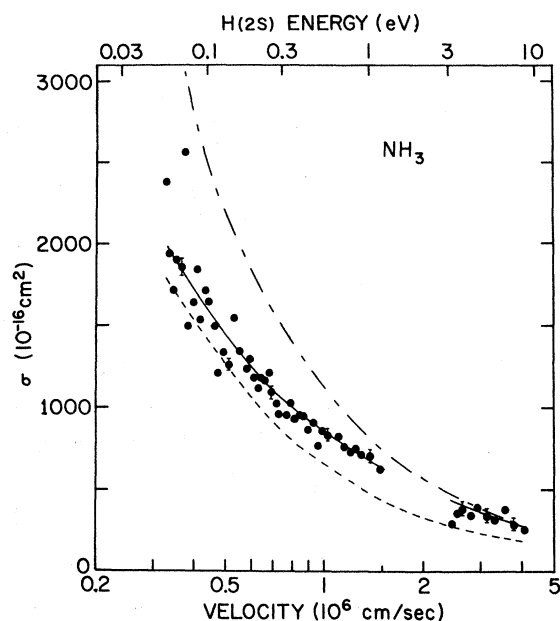
FIG. 12. Cross section for quenching in NH_3. The solid curve is a fit of Eq. (8) to the data. The dashed and broken curves are the prediction of the Slocomb, Miller, and Schaefer and the Gersten theory, respectively.
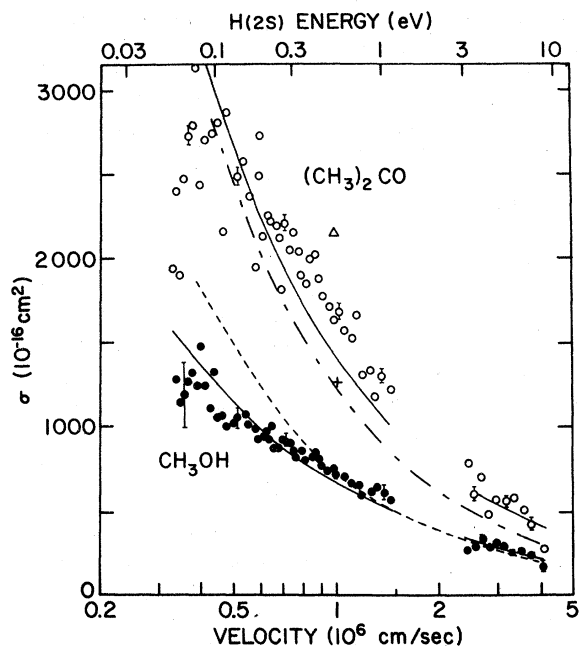
FIG. 13. Cross section for quenching in methanol (solid points) and acetone (circles). The solid curves through each set of data is a fit of Eq. (8) to the data. The dashed (broken) curve is the prediction of Slocomb, Miller, and Schaefer for methanol (acetone). The cross and triangle indicate the magnitude of Gersten's prediction for these two gases.

three pressures in addition to the zero-pressure data. The solid curves in the figures are a fit of Eq. (8) to the data, while the dashed curves show the cross section in the nonadiabatic limit, Eq. (2), using the Slocomb, Miller, and Schaefer value of Γ_1. The broken curve above the ammonia data gives Gersten's prediction for this gas, as do the cross and triangle above the methanol and acetone data.

The data for the dipole-moment molecules tends to favor the value of Γ_1 predicted by Slocomb, Miller, and Schaefer while Gersten's calculation of Γ_2 gives a better fit to the quadrupole-moment gases. Dose and Semini[12] report two calculations of Γ_1 in the Born and the Takayangi approximations which are 5% and 25% smaller than Gersten's Γ_1. None of these four calculations give values of both Γ_1 and Γ_2 consistent with the cross sections reported here.

There are two other cross sections reported in the literature for molecules with dipole moments. A velocity-averaged cross section for H_2O was reported by Fite et al.[7] and is 30% higher than the Slocomb, Miller, and Schaefer prediction. Dose and Hett[11] have made a study of quenching in methyliodide which agrees well with a v^{-1} velocity dependence and has a magnitude approximately 30% lower than the prediction of Slocomb, Miller, and Schaefer.

VI. CONCLUSIONS

The data reported here for the noble gases are in excellent agreement with the work of Kass and Williams over the velocity range covered in their work.[1,2] These two studies agree well with the measurements of Dose and Hett if their work is uniformly scaled by a factor of 1.15. This scale factor is independent of the nature of the quenching gas and the metastable velocity, except perhaps at the lowest velocities reported. This systematic discrepancy would suggest a calibration error such as in the determination of the effective density of the quenching gas.

A comparison of the three studies in the noble gases indicates that elastic scattering is not as important as predicted by Byron and Gersten. The present work, although an attenuation measurement like the others, treats elastic scattering in a different manner. The detection system used in this study has an effective angular acceptance for elastically scattered metastables which is approximately six times that used by Kass and Williams, and twice that of Dose and Hett. Thus the agreement between this study and the cross sections of Kass and Williams, as well as the similarity in the velocity dependence among the three

experiments, contradicts the large elastic scattering of the pseudopotential approach. The preliminary investigation of the ultraviolet-production cross section in argon reported here confirms this conclusion. The measurements of Dose and Hett in the noble gases tend to increase abruptly relative to the present work at the lowest velocities reported. This increase, particularly evident in xenon, may indicate that elastic scattering through angles greater than 90 mrad becomes important below 0.4×10^6 cm/sec. Dose cites evidence that supports this possibility.[14]

If the large-angle scattering is indeed small, then the quenching cross sections in the noble gases are considerably larger than predicted by either the pseudopotential approach or symmetric charge-exchange theory (in helium). Olson et al. have inverted the symmetric charge-exchange formalism and calculated the difference potential between the excited states of the HeH molecule and of the ArH molecule.[6] Presumably an improved pseudopotential is required in the Byron-Gersten theory.

A measurement of the collisional quenching of H(2S) and D(2S) in argon suggests that the cross sections differ by 8% at a velocity of 2×10^6 cm/sec, but are approximately equal when metastables with the same kinetic energy are compared. The agreement between the uv and attenuation-ratio cross sections would argue against elastic scattering as the source of the discrepancy.

There appears to be no single theoretical approach that correctly predicts the magnitude of the cross section for both dipole- and quadrupole-

moment molecules. The Slocomb, Miller, and Schaefer Born-approximation calculation, which works well for the molecules acetone, ammonia, and methanol, is too low for hydrogen and nitrogen. The Gersten calculation that successfully predicts the cross section for nitrogen is too low for hydrogen and too high in the dipole-moment gases. The problem is not likely to be due to elastic scattering; this conclusion is reached both on theoretical grounds and on the basis of the measurements of the relative cross section for the production of ultraviolet radiation. Measurements of this cross section in hydrogen by Dose and Hett, and in nitrogen reported here, require that nonradiative attenuation processes have the same velocity dependence as the uv cross section.

A comparison of the H_2 cross section with the noble-gas cross sections indicates that short-range forces are as effective as a small quadrupole moment in quenching metastable hydrogen atoms. This strongly suggests that the theory must include such short-range forces to allow a consistent treatment of both dipole- and quadrupole-moment molecules.

ACKNOWLEDGMENTS

*Work supported by AFOSR under Contract No. F44620-74-C-0081 and Grant No. 75-2864.

†Present address: Physics Department, University of Arizona, Tucson, Ariz. 85721.

‡Present address: University of California, Los Alamos Scientific Lab., Los Alamos, N. M. 87545.

§Present address: Molecular Physics Center, Stanford Research Institute, Menlo Park, Calif. 94025.

[1]R. S. Kass and W. L. Williams, Phys. Rev. Lett. 27, 473 (1971).

[2]R. S. Kass and W. L. Williams, Phys. Rev. A 7, 10 (1973).

[3]S. J. Czuchlewski and S. R. Ryan, Bull. Am. Phys. Soc. 18, 687 (1973).

[4]V. Dose and W. Hett, J. Phys. B 7, L79 (1974).

[5]F. Roussel, R. E. Olson, P. Pradel, A. S. Schlachter, G. Spiess, V. Dose, and W. Hett, in Abstracts of the Ninth International Conference on the Physics of Electronic and Atomic Collisions, edited by J. S. Risley and R. Geballe (University of Washington Press, Seattle, 1975), p. 243.

[6]V. Dose, W. Hett, R. E. Olson, P. Pradel, F. Roussel, A. S. Schlachter, and G. Spiess, Phys. Rev. A 12, 1261

(1975).

[7]W. L. Fite, R. T. Brackmann, D. G. Hummer, and R. F. Stebbings, Phys. Rev. 116, 363 (1959); R. F. Stebbings, W. L. Fite, D. G. Hummer, and R. T. Brackmann, Phys. Rev. 124, 2051(E) (1961).

[8]V. Dose and W. Hett, J. Phys. B 4, L83 (1971).

[9]S. J. Czuchlewski and S. R. Ryan, Bull. Am. Phys. Soc. 17, 1136 (1972).

[10]S. J. Czuchlewski, Ph.D. thesis (Yale University, 1973), available from University Microfilms, Ann Arbor, Michigan.

[11]V. Dose and W. Hett, in Abstracts of the Eighth International Conference on the Physics of Electronic and Atomic Collisions, edited by B. C. Čobić and M. V. Kurepa (Institute of Physics, Beograd, Yugoslavia, 1973), p. 857.

[12]V. Dose and C. Semini, in Ref. 11, p. 855.

[13]V. Dose and W. Hett, J. Phys. B 7, L454 (1974).

[14]V. Dose, Comments At. Mol. Phys. 5, 151 (1976).

[15]J. I. Gersten, J. Chem. Phys. 51, 637 (1969).

[16]C. A. Slocomb, W. H. Miller, and H. F. Schaefer III, J. Chem. Phys. 55, 926 (1971).

[17]F. W. Byron, Jr. and J. I. Gersten, Phys. Rev. A 3,

620 (1971).

[18]F. W. Byron, Jr., Phys. Rev. A **4**, 1907 (1971).

[19]F. W. Byron, Jr. and J. I. Gersten, Phys. Rev. Lett. **30**, 115 (1973).

[20]V. Dose, V. Meyer, and M. Salzmann, J. Phys. B **2**, 1357 (1969).

[21]F. W. Byron, Jr., R. V. Krotkov, and J. A. Medeiros, Phys. Rev. Lett. **24**, 83 (1970).

[22]H. B. Gilbody, R. Browning, R. M. Reynolds, and G. I. Riddell, J. Phys. B **4**, 94 (1971).

[23]G. Spiess, A. Valance, and P. Pradel, in *Abstracts of the Seventh International Conference on the Physics of Electronic and Atomic Collisions*, edited by L. M. Branscomb *et al*. (North-Holland, Amsterdam, 1971), p. 1083.

[24]H. B. Gilbody, R. Browning, R. M. Reynolds, and G. I. Riddell, in Ref. 23, p. 1080.

[25]R. V. Krotkov, F. W. Byron, Jr., J. A. Medeiros, and K. H. Yang, Phys. Rev. A **5**, 2078 (1972).

[26]H. B. Gilbody and J. L. Corr, J. Phys. B **7**, 1953 (1974).

[27]P. Pradel, F. Roussel, A. S. Schlachter, G. Spiess, and A. Valance, Phys. Lett. **50A**, 3 (1974).

[28]M. Leventhal, R. T. Robiscoe, and K. R. Lea, Phys. Rev. **158**, 49 (1967).

[29]S. J. Czuchlewski and S. R. Ryan, Bull. Am. Phys. Soc. **18**, 688 (1973).

[30]S. Czuchlewski, S. R. Ryan, and W. H. Wing, Rev. Sci.

Instrum. **47**, 1026 (1976).

[31]S. W. Duckett and P. H. Metzger, Phys. Rev. **137**, A953 (1965). See also J. E. Mack, F. Paresce, and S. Bowyer, Appl. Opt. **15**, 861 (1976); L. B. Lapson and J. G. Timothy, *ibid*. **15**, 1218 (1976).

[32]See, for example, K. Berkling, R. Helbing, K. Kramer, H. Pauly, C. Schlier, and P. Toschek, Z. Phys. **166**, 406 (1962).

[33]F. J. Comes and U. Wenning, Chem. Phys. Lett. **5**, 199 (1970).

[34]D. E. Stogryn and A. P. Stogryn, Mol. Phys. **11**, 371 (1966).

[35]F. J. Comes and U. Wenning, Z. Naturforsch. **24A**, 587 (1969).

[36]J. E. Mentall and E. P. Gentieu, J. Chem. Phys. **52**, 5641 (1970).

[37]For example, the reaction $H(2S) + H_2 \rightarrow H_3^+ + e^-$ has been considered by W. A. Chupka, M. E. Russell, and K. Refaey [J. Chem. Phys. **48**, 1518 (1968)] who conclude that it is exothermic with a cross section on the order of 10^{-16} cm^2 at 10^6 cm/sec and varies as $1/v$. If this estimate is correct, the process is not important in quenching metastables.

[38]R. D. Nelson, D. R. Lide, Jr., and A. A. Maryott, *Selected Values of Electric Dipole Moments for Molecules in the Gas Phase*, Natl. Stand. Ref. Data Ser. Natl. Bur. Stand. No. 10 (U.S. GPO, Washington, D.C., 1967).